Geochemistry Geophysics Geosystems G3
AN ELECTRONIC JOURNAL OF THE EARTH SCIENCES
Published by AGU and the Geochemical Society

Article
Volume 9, Number 7
26 July 2008
Q07023, doi:10.1029/2008GC002038
ISSN: 1525-2027

Terrigenous events and climate history of the Sophia Basin, Arctic Ocean

Daniel Winkelmann
Alfred Wegener Institute for Polar and Marine Research, Columbusstrasse, D-27568 Bremerhaven, Germany

Now at Leibniz Institute for Marine Sciences, Wischhofstrasse 1-3, D-24148 Kiel, Germany (dwinkelmann@ifm-geomar.de)

Christoph Schäfer, Rüdiger Stein, and Andreas Mackensen
Alfred Wegener Institute for Polar and Marine Research, Columbusstrasse, D-27568 Bremerhaven, Germany

[1] Periods of enhanced terrigenous input to the ocean's basins of the North Atlantic have been reported for the last glacial period. We present a set of new sediment cores recovered from the Sophia Basin north of Svalbard which exhibit widespread ice-rafted debris layers reflecting enhanced terrigenous input throughout the last ~200 ka B.P. Their consistent stratigraphic position, sedimentological character, high sedimentation rate, and geochemical characteristic point to synchronously deposited layers which we name terrigenous input events (TIEs). Owing to their higher densities, they generate excellent reflectors for sediment-penetrating acoustic devices and prominent acoustic layers in the imagery of sedimentary structures. Therefore TIEs can be used for regional acoustic stratigraphy. Each of the events can be linked to major glacial activity on Svalbard. However, the Early Weichselian glaciation is not recorded as a TIE and, in agreement with other work, might not have occurred on Svalbard as a major glacial advance to the shelf break. Nonsynchronous timing of western and northern sources on Svalbard points against sea level–induced iceberg discharge events.

Components: 7104 words, 8 figures, 2 tables.

Keywords: Sophia Basin; Svalbard; Arctic Ocean; Quaternary climate history; organic carbon; glacial activity.

Index Terms: 3002 Marine Geology and Geophysics: Continental shelf and slope processes (4219); 1621 Global Change: Cryospheric change (0776); 1050 Geochemistry: Marine geochemistry (4835, 4845, 4850).

Received 27 March 2008; **Accepted** 6 May 2008; **Published** 26 July 2008.

Winkelmann, D., C. Schäfer, R. Stein, and A. Mackensen (2008), Terrigenous events and climate history of the Sophia Basin, Arctic Ocean, *Geochem. Geophys. Geosyst.*, *9*, Q07023, doi:10.1029/2008GC002038.

1. Introduction

[2] Periods of enhanced terrigenous input to the ocean's basins of the North Atlantic have been reported for the last glacial period [*Heinrich*, 1988; *Bond et al.*, 1992]. These IRD-rich Heinrich layers have been associated with events of excessive iceberg discharge from the Laurentide ice sheet [*Bond and Lotti*, 1995] and related to internal ice sheet dynamics [e.g., *MacAyeal*, 1993] as well as external forcings [*Bond and Lotti*, 1995; *Fronval et al.*, 1995]. Owing to their detrital carbonate contents derived from outcropping carbonates in the

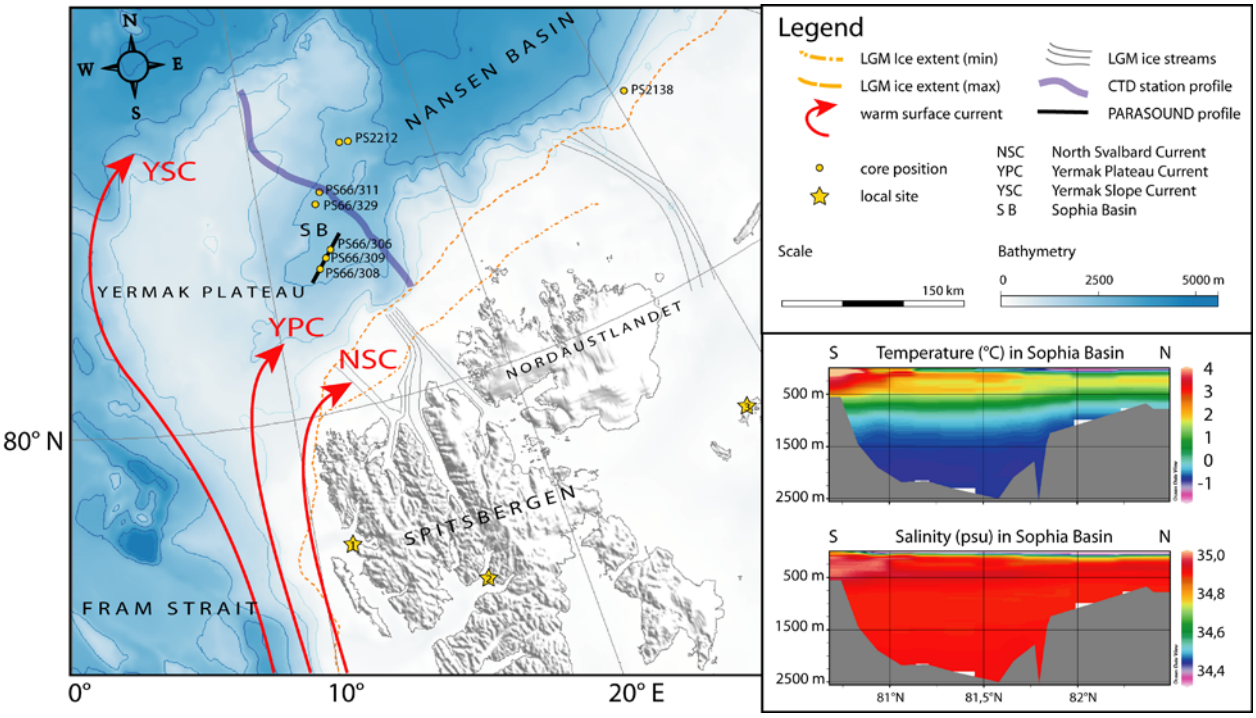

Figure 1. Location map with core stations and PARASOUND profile. LGM extent according to *Landvik et al.* [1998], ice streams according to *Ottesen et al.* [2005], Atlantic water advection indicated as surface branches of the West Spitsbergen Current (including CTD profile) according to *Schauer et al.* [2004], bathymetry from IBCAO [*Jakobsson et al.*, 2000]. Terrestrial sites: 1, Brøggerhalvøya; 2, Kapp Ekholm; 3, Hidalen (on Kongsøya).

drainage area, these layers can be recognized as Ca/Sr peaks in XRF analysis [*Hodell et al.*, 2005].

[3] In contrast to Greenland [cf. *Kierdorf*, 2006], Spitsbergen represents a source for terrigenous organic carbon in modern sediments [*Winkelmann*, 2003; *Winkelmann and Knies*, 2005], and organic carbon related parameters (aside others) can be used as a marker for this terrigenous input.

[4] Here we present a new set of sediment cores recovered from the Sophia Basin north of Svalbard in 2004 (Figure 1) exhibiting widespread layers of enhanced terrigenous input throughout the last ~200 ka B.P. On the basis of a suite of geochemical parameters (including TOC, C/N, Zr/Ca), we show that these Heinrich-like layers can be related to glacial activity and thus to the Quaternary glaciation history of the Svalbard archipelago and the Svalbard-Barents Sea Ice Sheet (SBIS).

2. Material and Methods

[5] Detailed bathymetric data and high-resolution ground-penetrating echo-sounding data were acquired by the HYDROSWEEP DS2 and the PARASOUND Hydromap Control systems, respectively, aboard R/V *Polarstern* during cruise ARKXX/3 [*Stein*, 2005]. Additional data from cruise ARKXV/2 of R/V *Polarstern* [*Jokat*, 2000] have been compiled to analyze the area and structure of the Hinlopen/Yermak Megaslide [*Winkelmann et al.*, 2006a, 2006b; *Winkelmann and Stein*, 2007]. On the basis of this synthesis, coring sites have been carefully selected along PARASOUND profiles crossing the well-developed marginal facies of the mega slide during cruise ARKXX/3 [*Stein*, 2005]. A total number of 14 gravity cores were taken from key locations. Beside the standard gravity coring equipment the giant gravity corer (kastenlot, 30 × 30 × 1500 cm) has been applied to yield sufficient sedimentary material for dating from key sites [*Stein*, 2005]. Multisensor core logging (MSCL), opening of cores, core description, X-ray radiography and standard sampling have been performed aboard R/V *Polarstern*.

[6] We chose two cores, PS66309-1 KAL and PS66/308-3 SL, as key cores for the paleoceanographic characterization. Both cores are undisturbed except for the slide-related marginal turbidite (which they were intended to recover [cf. *Winkelmann et al.*, 2006a; *Winkelmann and Stein*, 2007]). Recovered ~10 km away from each other, they show an excellent correlation of all

Table 1. Gravity Cores of This Study

Core	Latitude	Longitude	Water Depth (m)	Recovery (cm)	Type
PS66/306-2	81° 14.5′N	13° 18.6′E	2268	350	gravity core
PS66/308-3	81° 07.3′N	12° 35.9′E	2218	554	gravity core
PS66/309-1	81° 11.2′N	12° 59.1′E	2269	765	giant gravity core (kastenlot)
PS66/311-2	81° 41.8′N	13° 28.2′E	2192	493	gravity core
PS66/329-3	81° 36.3′N	13° 6.1′E	2211	482	gravity core

measured parameters confirming a joint history of paleoenvironmental changes. We selected PS66/329-3 SL and PS66/311-3 SL in addition for representation of the NW Sophia Basin and PS66/306-3 SL for completion of the key profile (Figure 1 and Table 1).

[7] Core PS66/309-1 was sampled continuously at 2–3 cm intervals for tests of *Neogloboquadrina pachyderma* (*sin.*). Stable oxygen ($\delta^{18}O$) and carbon ($\delta^{13}C$) isotopes were measured by standard techniques [*Duplessy*, 1978] on the automated Carbo-Kiel device connected to a Finnigan MAT 251 mass spectrometer at the Alfred Wegener Institute (AWI) in Bremerhaven, Germany. The external analytical reproducibility is 0.08‰ and 0.06‰ for $\delta^{18}O$ and $\delta^{13}C$, respectively. Total carbon (TC), total organic carbon (TOC) and total nitrogen (N_{tot}) were determined by means of a LECO CS 125 and CNS 2000 analyzer [*Schäfer*, 2005], and carbonate calculated as $CaCO_3$ = (TC − TOC) * 8,33. IRD was counted according to *Grobe* [1987] as lithic particles from the X-ray radiographies.

[8] X-ray fluorescence analysis was performed on an Avaatech automated (XRF) core scanner [*Richter et al.*, 2006] at the AWI, Bremerhaven. Split core segments were scanned at 10 and 30 KV. The standard model for marine sediments (including Al, Si, P, S, Cl, K, Ca, Ti, Cr, Mn, Fe, Co, Rh, Ba, Cu, Zn, Ga, Br, Rb, Sr, Y, Zr, Au, Pb, Bi) was used for calculation of elemental activities [*Winkelmann*, 2007]. A density correction for light elements (Al, Si) of the core top [cf. *Tjallingii et al.*, 2007] was not applied owing to our focus on heavier elements and the deeper core record.

[9] AMS radiocarbon dating was performed on carbonaceous shells of *N. pachyderma sinistralis* at the Leibniz Laboratory for Radiometric Dating and Isotope Research at the Christian Albrecht University in Kiel, Germany. ^{14}C ages have been converted to calendar ages using the CalPal online software (http://www.calpal-online.de) with the CalPal2005_SFCP calibration curve and a correction for the reservoir effect of 420 years [*Winkelmann et al.*, 2006a; *Winkelmann and Stein*, 2007]. All data are available online via http://www.pangaea.de (doi:10.1594/PANGAEA.695687).

3. Applied Paleoproxies

[10] Following our initial sedimentological and physical examination of the TIEs, we further applied conventional C/N and Zr/Ca ratios from XRF scanning to further characterize these events.

[11] C/N ratios have been used since long for reconstructions of paleoenvironments in the study area [e.g., *Stein et al.*, 1994; *Knies and Stein*, 1998; *Mangerud et al.*, 1998; *Knies et al.*, 1999, 2000; *Stein and Mcdonald*, 2004]. Their interpretation has been questioned owing to the fact that inorganic nitrogen bound to the lattice structure of clay minerals would dilute the C/N signal [e.g., *Schubert and Calvert*, 2001]. From an earlier study [*Winkelmann*, 2003; *Winkelmann and Knies*, 2005] it can be seen that conventional bulk C/N (TOC/N_{tot}) ratios correlate well to the corrected organic C/N (TOC/N_{org})(R^2 = 0, 91; n = 45) as well as to the $\delta^{13}C_{org}$ signal (R^2 = 0, 66; n = 45) (Figure 2). Thus, *Winkelmann* [2003] and *Winkelmann and Knies* [2005] showed too that conventional C/N ratios not only remain an important paleoproxy in the Svalbard/Fram Strait area, but that they mark central Spitsbergen as a significant source for this TOM supply. The C/N aside TOC/N_{org}, $\delta^{13}C_{org}$ and $\%N_{org}$ (or $\%N_{inorg}$) trace this input along the Isfjorden, Van Mijen Fjorden and Storfjorden. The problem of diluting the C/N signal by terrigenous nitrogen (bound as ammonium to the lattice structure of clay minerals) is less important because the measured C/N would only underestimate the terrestrial input leaving the prominent C/N peaks (in our core records) unaffected by the interpretation of enhanced terrigenous input of organic matter.

[12] In addition to the C/N ratios we applied Zr/Ca ratios that phenomenologically record the TIEs. We interpret Zr to reflect detrital zircons derived from drainage areas of northern Svalbard. This hinterland is dominated by igneous and metamorphic rocks and Devonian polimict conglomerates crop

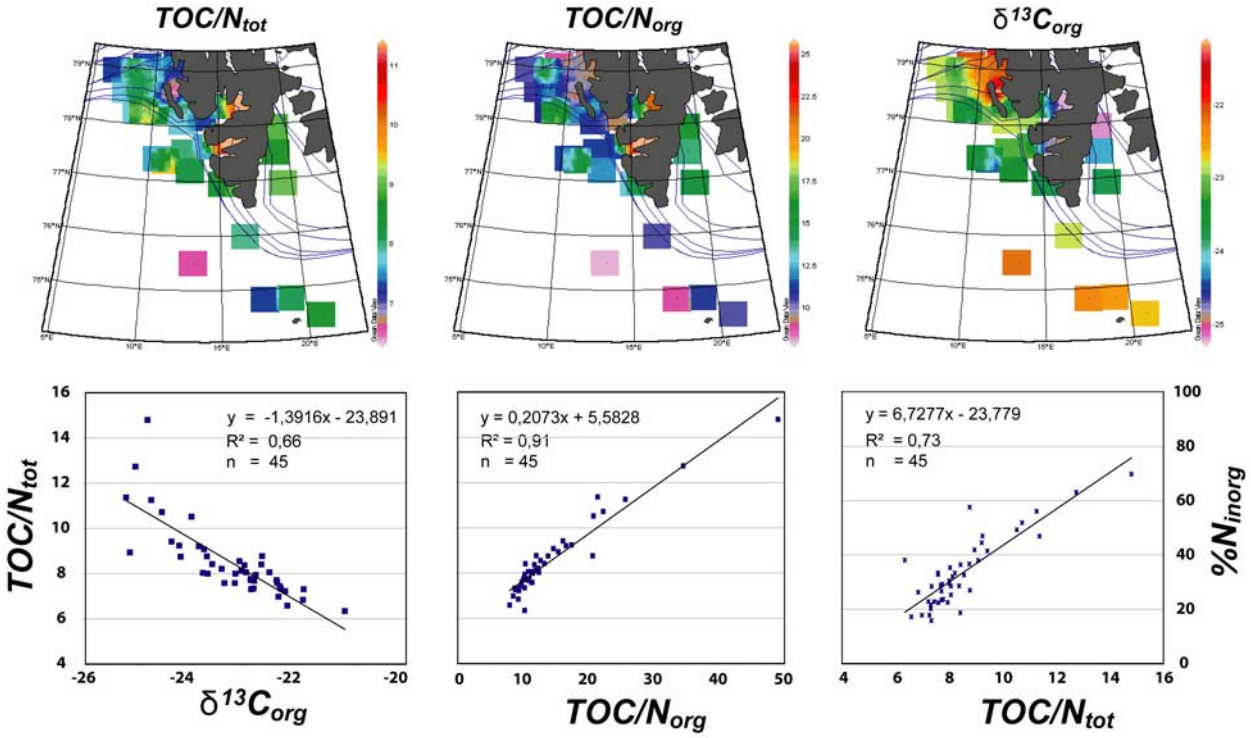

Figure 2. Correlation of conventional TOC/N_{tot} versus $\delta^{13}C_{org}$, TOC/N_{org}, and percentage of inorganic nitrogen bound as ammonium to the lattice structure of clay minerals ($\%N_{inorg}$) from surface sediment samples around Spitsbergen (data from *Winkelmann and Knies* [2005]).

out only along the Billefjorden on a larger scale. Therefore, we assume the source-specific character of the Zr signal in the Sophia Basin. We put the Zr in relation to Ca as indicator for terrigenous input. We interpret the Ca record to be mainly controlled by productivity and dilution. The intrinsic assumption of a marine carbonate is based on the following facts: First, a one-to-one correlation of bulk carbonate record (calculated for $CaCO_3$) and the measured Ca activities meaning no indication of (detrital) dolomite [cf. *Vogt et al.*, 2001]. Second, the synoptic presence of (partly abundant) foraminifers throughout the core except for the TIEs (there present but extremely diluted); consistent with the bulk carbonate and Ca records as well as with findings of *Knies et al.* [2003]. In addition, the TIEs being clearly of terrigenous origin, exhibit lowest (down to no) carbonate contents. Sparse foraminifers could even been found within the TIEs pointing to dilution rather than dissolution. No detrital carbonates (clasts, pebbles, etc.) have been found during sampling and other core examinations.

[13] We are aware that this source-specific assumption of the Zr/Ca ratio comes with uncertainties like grain size dependency. However, most established proxies show a relationship to grain size owing to the fact that their mineral or detrital carrier is preferentially found in a certain grain size spectrum. How much the Zr/Ca ratio can be affected by grain size can be assessed within the turbidite. However, being well sorted, the turbidite contains high amounts of eroded, reworked foraminiferal shells that are responsible for the high carbonate values. This complicates a direct comparison. The TIEs clearly show higher grain sizes which in itself can be the reason for the higher Zr contents. However, if the higher Zr contents are mainly controlled by grain size they still characterize and thus record the TIEs. Thus, differential timing of Zr/Ca and C/N peaks in our records can be interpreted as different timing of sources.

4. Results

[14] Distinct layers with higher proportions of terrigenous material are present in all sediment cores at the same stratigraphic position. We name them terrigenous input events (TIEs) that are identified in detail by the following.

4.1. Sedimentological Characteristic

[15] The TIEs are layers of generally coarser grain size. This means gravelly sand or sandy layers with

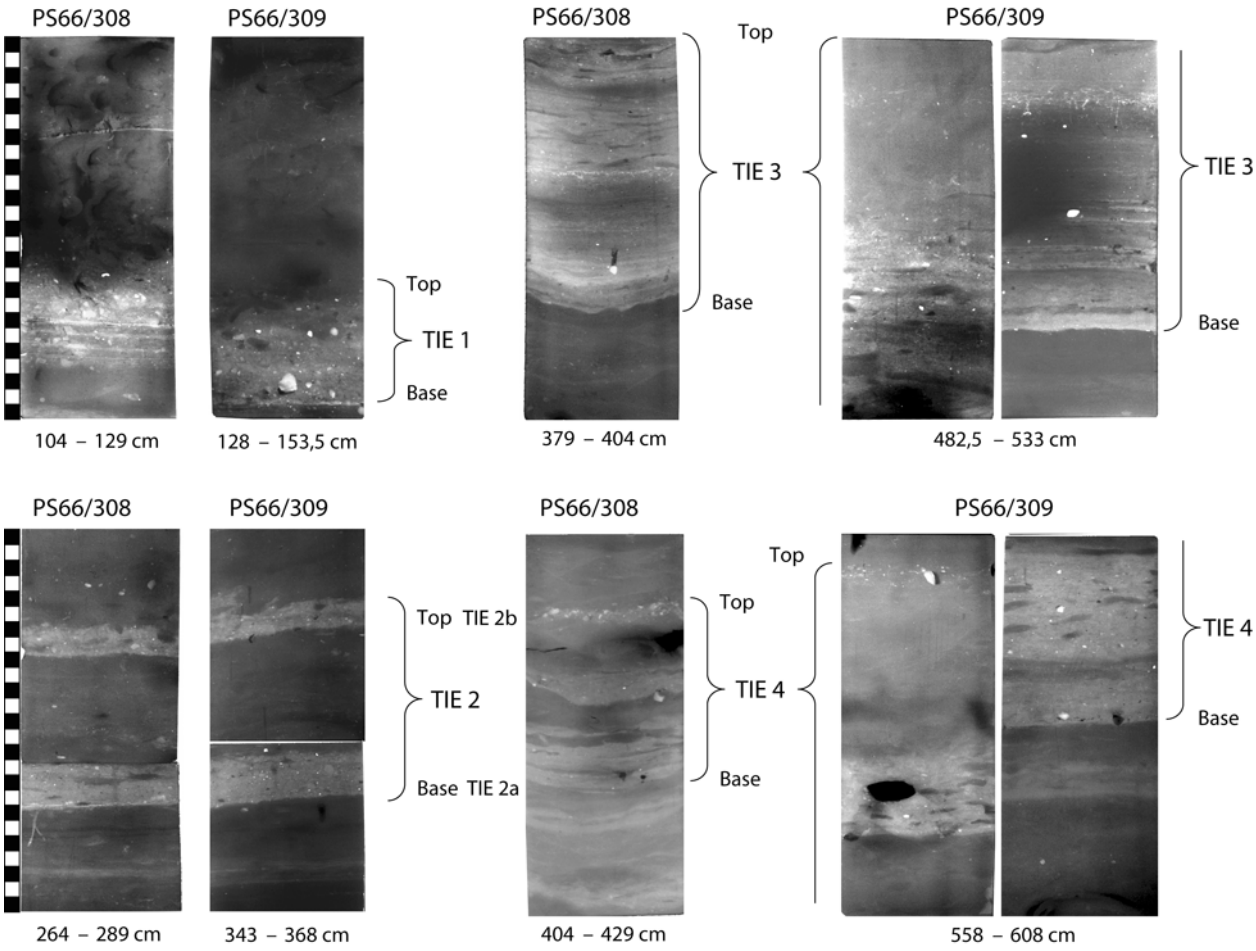

Figure 3. X-ray radiographs from terrigenous input events (TIEs) 1 to 4 of the key cores PS66/308 and PS66/309. The TIEs are generally characterized by enhanced IRD input and associated coarser grain sizes (coarse silt, sand, and gravel), embedded mudclasts, and high sedimentation rates (inferred from pulse-like layering (see TIE 1 in PS66/308)). Note that the TIEs do correspond to pronounced IRD layers but can include an interval of virtual little or no IRD input (TIE 2).

individual pebbles. In this they represent layers of enhanced accumulation of IRD. The IRD signal as applied here (counted grains bigger than 1 mm diameter per 10 ccm of sediment according to *Grobe* [1987]) does not fully reflect these layers. They partly exhibit lamination (e.g., TIE 0, TIE 1 in PS66/308; Figure 3). This points to a rapid sedimentation with a pulse character. Other reasons for lamination like seasonality, anoxic conditions, etc. are excluded. Bioturbation can be seen from the top of some laminated layers penetrating into them, identifying a period of reduced sedimentation after a pulse (e.g., within TIE 3; Figure 3). Fining upward (intraunit, partly well developed, and less well developed, gradational toward their tops) characterizes them again as pulses of enhanced sedimentation.

[16] From this synoptic examination we can characterize the TIEs as layers of enhanced input of ice-rafted terrigenous debris (strictly speaking, IRD).

4.2. Geochemical Properties

[17] The TIEs are all characterized by C/N ratios above 8 and peak TOC (>0.6 wt.%) concentrations. They exhibit minimum carbonate contents as seen in the calculated $CaCO_3$ bulk and scanned Ca record. Further, they host higher contents of Zr. In consequence, they appear as distinct peaks in the Zr/Ca (>0.2) record, pointing to higher siliciclastic proportions (Figure 4).

4.3. Physical Properties

[18] The physical properties of the TIEs include higher densities (above 1.65 g/ccm; Figures 4 and 5),

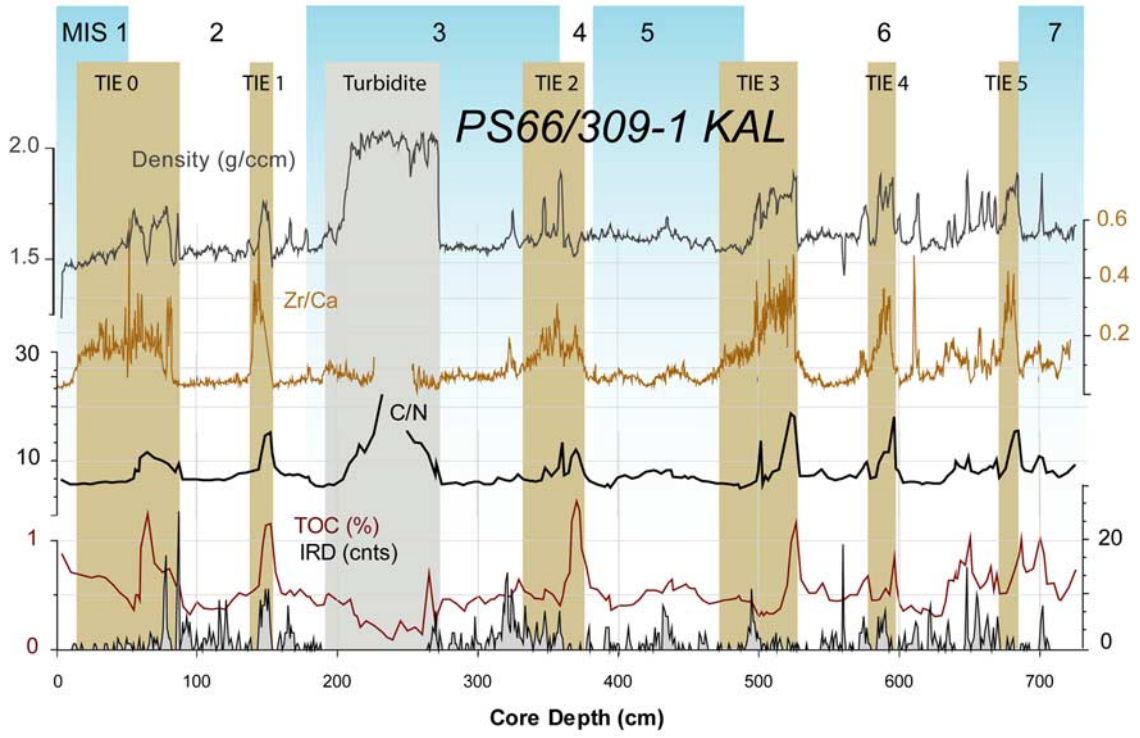

Figure 4. Terrigeneous events (brown boxes) within the Sophia Basin in key core PS66/309-1. Core record of density log (MSCL), geochemical bulk parameters (TOC, C/N), XRF-elemental ratio (Zr/Ca), and IRD including indication of slide-related lithological units (marginal turbidite; gray box). The peaks of the Zr/Ca ratio indicate increased input of detrital terrigenous minerals (zircon), from outcropping lithological strata on Svalbard. Thus, the Zr/Ca ratio, here, can be used as proxy for glacial activity. Event 0 reflects Termination I; Event 1 (E1) reflects the Late Weichselian glacial advance to the shelf edge; Event 2 (E2) reflects the onset and termination of the Mid Weichselian glaciation; Event 3 (E3) reflects Termination II; and Event 4 (E4) reflects the Late Saalian glacial advance to the shelf edge during MIS 6.2. Further events within MIS 6 (e.g., Event 5, etc.) have not been named since they are less consistently recorded in our sediment cores. Note the signal offsets between C/N and Zr/Ca ratios, indicating different timing of the individual sources (west Spitsbergen and Storfjord Trough for C/N [cf. *Winkelmann and Knies*, 2005] and NE Svalbard for the Zr/Ca ratios).

higher acoustic impedance and in their upper parts a slightly higher magnetic susceptibility (due to decreasing grain size). The TIEs generally show lower RGB color values reflecting their grayish color.

4.4. Acoustic Properties

[19] The relation of contrasts in acoustic impedance and density to acoustic reflectors has been shown earlier for the Sophia Basin [e.g., *Winkelmann et al.*, 2006b]. As a consequence of their higher acoustic impedance (see above), and the contrast in acoustic impedance to the underlying and overlying strata (about 400 units higher than the average background values) and their consistent surface character, the TIEs form pronounced acoustic reflectors in a suitable (sufficient resolution and penetration) sediment-penetrating sonar system (Figure 6). Especially the high-resolution PARASOUND system aboard R/V *Polarstern* records these layers with high precision. With the establishment of our chronology, they can be, thus, used for acoustic stratigraphy in a regional context.

4.5. Consistent Stratigraphic Position

[20] On the basis of our sediment cores and coverage by PARASOUND data throughout the Sophia Basin, we can see that the TIEs occur without exception in the megaslide-unaffected parts of the basin. Moreover, they can be traced by PARASOUND data from core to core. Within the sediment cores TIEs can clearly be identified by their darker, grayish color and the same down core sequence.

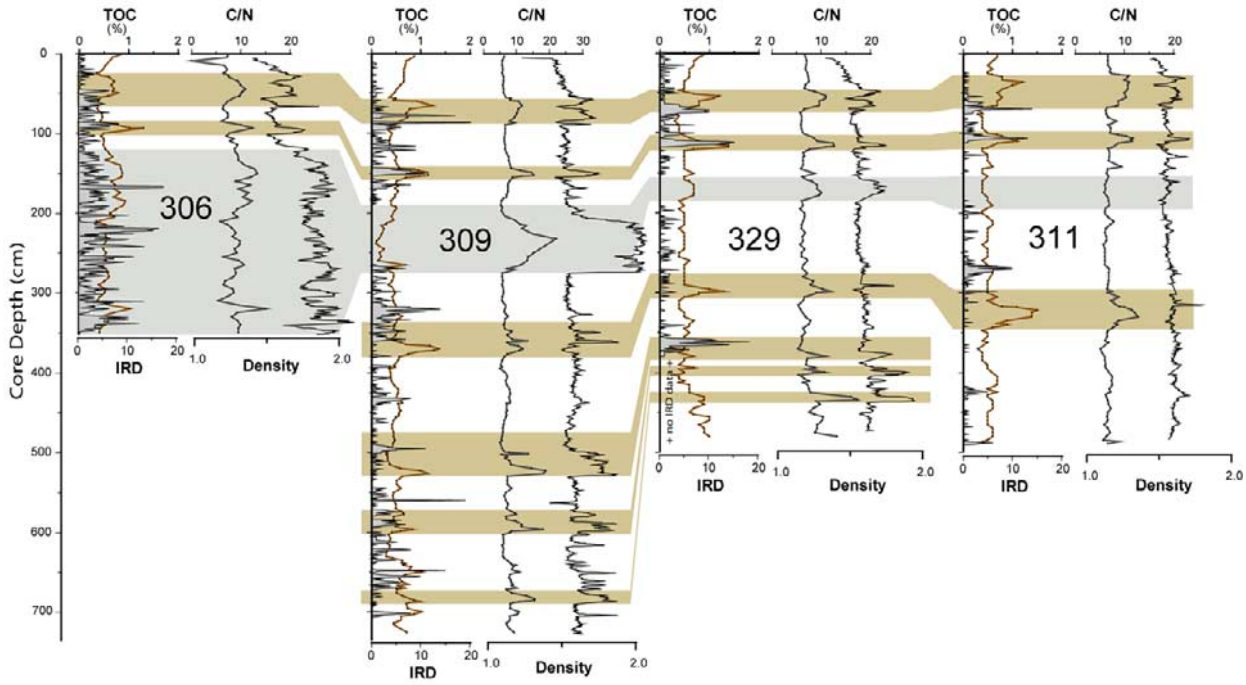

Figure 5. Key core PS66/309-1 and correlation to bulk and MSCL data in the west Sophia Basin [*Winkelmann et al.*, 2008]. Brown boxes indicate TIEs; gray boxes indicate the slide-related lithologies (debris flow, turbidite, fining upward).

[21] This consistent stratigraphic position, corroborated by PARASOUND data and an excellent correlation to other dated cores (PS1533, PS2212, PS2128), made us feel confident in assuming them to represent synchronously deposited layers. The high sedimentation rates with pulse character as seen from our sedimentological examination of X-ray radiographies corroborates the interpretation of rapidly and synchronously deposited layers.

5. Stratigraphy

[22] The stratigraphy of our cores is based on the high-resolution record of stable isotopes (*N. pachyderma sin.*) which were correlated to the global isotope curve SPECMAP stack [*Martinson et al.*, 1987] and several radiocarbon dates of the key core PS66/309-1 [*Winkelmann*, 2007] (Figure 7). Ages of MIS boundaries and events have been corrected according to *Lisiecki and Raymo* [2005] and *Thompson and Goldstein* [2006]. Four AMS ^{14}C dates of *N. pachyderma* (*sin.*) [*Winkelmann et al.*, 2006a, 2006b] helped to pinpoint MIS 2 and 3 and one has been correlated from core PS1533-3 [*Spielhagen et al.*, 2004] to pinpoint MIS 1 (Table 2).

[23] Well-dated melting events during Termination I, e.g., at 14.5 ^{14}C ka B.P., have been recognized in the adjacent areas [cf. *Hebbeln et al.*, 1994]. In core PS66/309 a series of meltwater peaks characterize the MIS 2. We date the most prominent peak at 15.66 ± 70 ^{14}C ka B.P. (18,491 ± 237 cal. ka B.P.). The MIS 3/2 boundary is characterized by a well-defined sequence of sedimentological, mineralogical and organic-geochemical parameters in all sediment cores in the region [cf. *Andersen et al.*, 1996; *Vogt et al.*, 2001]. The middle part of this interval exhibits lamination and contains high amounts of mature terrestrial organic material (Figures 3, 4, and 5) and, among other, very low carbonate contents [*Vogt et al.*, 2001]. This layer was described as Event I by *Knies and Stein* [1998] and corresponds to TIE 1. It was deposited between 22.5 and 19.5 ^{14}C ka B.P. as based on several AMS ^{14}C ages. In core PS66/309-1 KAL the closest AMS ^{14}C date directly above this layer gives an age of 20.02 ± 140 ^{14}C ka B.P. (23379 ± 394 cal. ka B.P., Table 2 and Figures 2 and 3). Assuming it to be a synchronous deposit in all sediment cores we use it as one indicator of the lowermost MIS 2. However, following the age correction of *Lisiecki and Raymo* [2005], the MIS2/3 boundary is best defined by our closest AMS date (Table 2). The MIS3/4 boundary is based upon an increase to peak values in δ^{13}C in the early MIS 3 shortly after a typical peak in the

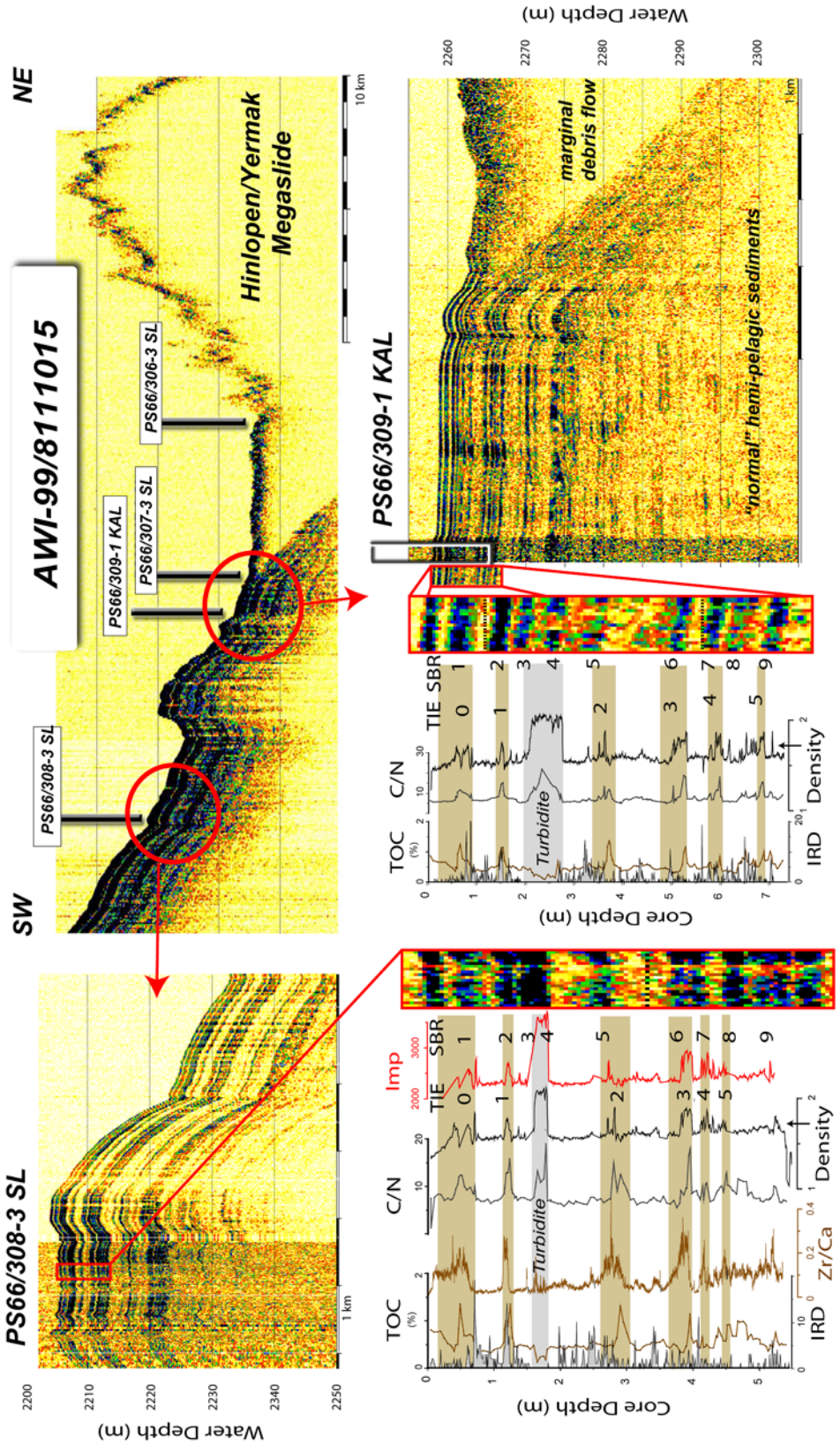

Figure 6. Key profile AWI-99/8111015 of shallow seismic (PARASOUND) across the megaslide margin in the SW Sophia Basin. IRD, bulk geochemical records, and MSCL data of key cores PS66/309-1 and PS66/308-3 (including impedance and Zr/Ca from XRF analysis) and their correlation to PARASOUND [*Winkelmann et al.*, 2006a]. Each terrigenous input event (TIE) creates a subbottom reflector (SBR) in the PARASOUND image. Note that the differences in core depths of the layers and their thickness in core 308 (standard gravity corer) indicate intensive compaction during coring. Compaction and subbottom depth differences (PARASOUND versus sediment core) are lowest when the giant gravity corer (kastenlot) is applied.

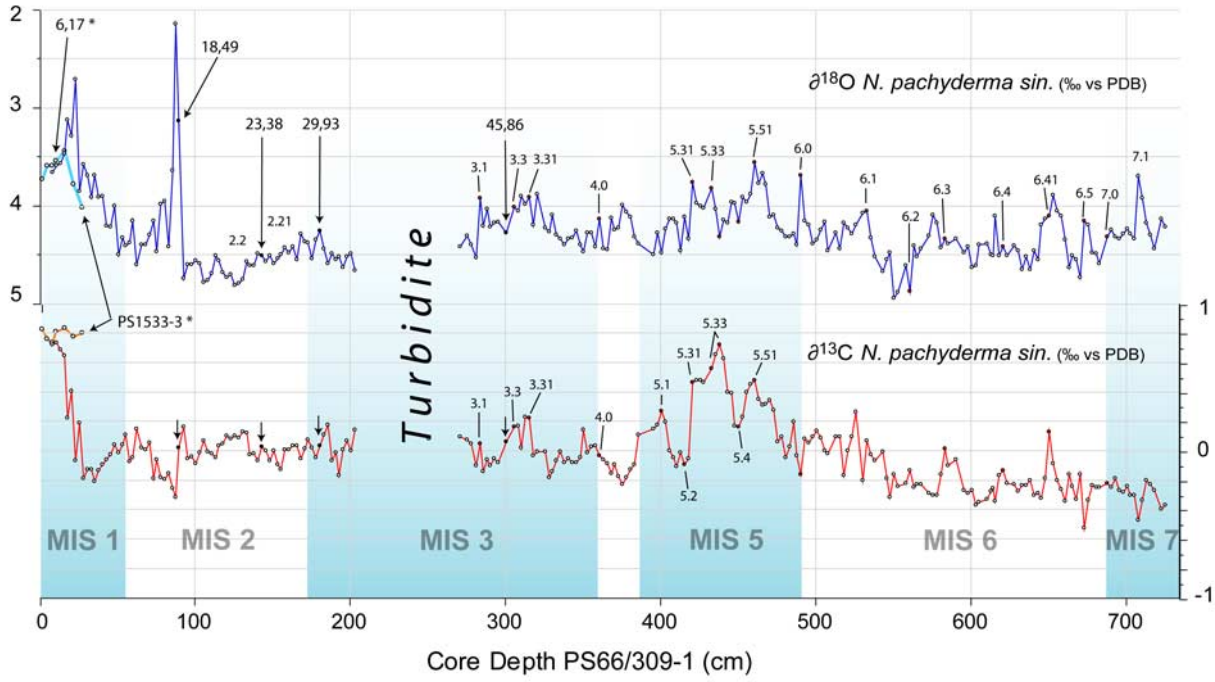

Figure 7. Stable isotopic record (*Neogloboquadrina pachyderma sinistralis*), AMS radiocarbon dates, and chronology of the key core PS66/309-1. Assignment of isotope stages according to *Martinson et al.* [1987].

C/N ratios that is not reflected in the TOC signal and the onset of intensive ice rafting at the MIS4/3 boundary. This interval is characterized by a carbonate minimum too. A typical decrease of the $\delta^{13}C$ values from late MIS 5 to lowest values in early MIS 4 is observed and used as a regional stratigraphic fix point for the MIS4/5 boundary [cf. *Dokken and Hald*, 1996; *Nørgaard-Pedersen et al.*, 1998; *Spielhagen et al.*, 2004]. The MIS5/6 boundary is based on the $\delta^{18}O$ meltwater peak that is accompanied by peak IRD concentration shortly after a characteristic C/N peak (that again is not reflected in the TOC record), a distinct carbonate minimum and a density maximum, indicating Termination II. The definition of MIS boundaries is further supported by the correlation to the Greenlands ice core data (N-GRIP and GRIP) [*Winkelmann*, 2007], by correlation to PS2212 [*Vogt et al.*, 2001; cf. *Winkelmann*, 2007] and PS2644 which has been correlated to the GRIP record in great detail [*Voelker*, 1999; *Voelker et al.*, 2000; cf. *Winkelmann*, 2007].

[24] The stratigraphic model for the sediment cores from transects across the Hinlopen/Yermak Megaslide's western margin in Sophia Basin has been established by correlation of MSCL data to PS66/309-1 KAL [*Winkelmann et al.*, 2006a, 2006b, 2008]. This correlation is further supported by correlation of geochemical bulk and IRD records (Figure 4) and acoustic reflection data (see below).

[25] According to our chronology, the TIEs correspond to Termination 1 (TIE 0), the approaching of the shelf break during LGM onset (TIE 1; identical with Event 1), the onset and termination of the Mid Weichselian glaciation (TIE 2; or 2a and 2b, respectively; see Figure 3), Termination 2 (TIE 3) and the onset of the Late Saalian glaciation (TIE 4). There are earlier events (e.g., TIE 5) that might correspond to the onset of an Early Saalian glaciation. However, the following termination (not labeled, Figure 5) is less consistently recorded. Owing to this and decreasing stratigraphic control, we refused to outline and discuss them further.

6. Discussion

[26] *Winkelmann* [2003] and *Winkelmann and Knies* [2005] have shown that a distinction between marine and terrigenous organic carbon on the Spitsbergen shelf based on geochemical bulk parameters is possible. The stable carbon isotopic composition of the organic carbon fraction ($\delta^{13}C_{org}$) aside HI, T_{max} (Rock-Eval pyrolysis) and elemental C/N ratios (C/N, TOC/N_{org}),

Table 2. Age Fix Points of Refined Age Models for Both Cores[a]

Age (cal. ka B.P.)	MIS*	PS66/309-1 (cm Core Depth)	PS66/308-3 (cm Core Depth)	Reference
10.9		***15.5***		***6***
18.49	-	***89.5***	72.6	4
23.38	-	***143***	111.2	5
29.93	-	***180.5***	141.8	4
31.1	3.1	283.0		1
45.86	-	***300.5***	216.8	4
47.8	3.3	305.5	224.8	1
52.2	3.31	315.5	234.8	1
57	4.0	360.0	279.8	2
67.7	4.23	385.0	290.4	1
71	5.0	385.5	299.0	2
80.5	5.1	400.5	312.2	1
91.3	5.2	415.5	324.6	1
100.3	5.31	420.5	330.8	1
104.0	5.33	433.0	335.0	1
108.5	5.4	450.5	351.4	1
122.6	5.51	460.5	357.8	1
129.3	6.0	490.5	381.4	1
135	6.2	560.5	408.0	3
142	6.3	583.0	416.0	3
153.9	6.4	620.5	428.8	1
164.0	6.41	650.5	441.6	1
172.9	6.5	673.0	451.4	1
179.2	7.0	688.0	457.2	1
190.8	7.1	708	463.8	1

[a] AMS radiocarbon dates from PS66/309-1 were correlated to PS66/308-3 by their Ca and carbonate records. References for MIS event ages: 1, *Thompson and Goldstein* [2006]; 2, *Lisiecki and Raymo* [2005]; 3*, SPECMAP event numbers from *Martinson et al.* [1987]; 4, AMS radiocarbon dates (bold italic) from *Winkelmann et al.* [2006a]; 5, *Winkelmann and Stein* [2007]; 6, *Spielhagen et al.* [2004].

appeared most favorable for this distinction. However, the standard application of conventional C/N ratios for a general determination of terrigenous input of organic matter proved to be valuable (Figure 2) though not to be useful for budgeting of organic carbon proportions.

[27] The higher input of terrigenous organic material from Svalbard is reflected among others in the C/N ratios [cf. *Winkelmann*, 2003; *Winkelmann and Knies*, 2005]. Mineralogic evidence (orderly layered expandable minerals, OLEMs) for some TIE-internal layers points to a Storfjord Trough origin [*Vogt et al.*, 2001]. Every TIE starts with a distinct peak in TOC and C/N. Followed by peaks in the Zr/Ca ratios that last about 2 ka and decline gradually toward normal values. The offset between C/N ratios (reflecting west Spitsbergen and Storfjord) and Zr/Ca ratios (reflecting north Svalbard) points to a different regional glaciation timing on Svalbard (Figure 4). Consequently, the western fjords of Spitsbergen and the Storfjord Trough are first active and their drainage areas are, thus, more sensitive for glacial inception. The northern Svalbard sources with lower TOC and higher siliciclastic composition [cf. *Winkelmann*, 2003; *Winkelmann and Knies*, 2005] respond more slowly or retarded both, during inception and during termination of a major glaciation. All of the 5 TIEs can be related to major glacial activity on Svalbard.

[28] There is only one event between TIE 5 and 4 (not labeled) that is less consistently recorded (Figures 4 and 5). A plausible explanation is that MIS 6 was generally characterized by heavier stable oxygen isotopic values (i.e., colder) (Figure 7). Therefore the glaciated Arctic archipelago might have been responded less effective to an ice sheet decay. The sedimentation pattern resembles the period between MIS 4 and 3 with interstadial-like characteristics before TIE 4 although on a ''colder level'' [cf. *Winkelmann*, 2007]. However, the missing sedimentological evidence of enhanced terrigenous input in our sediment cores throughout the early Weichselian (circa 120–100 cal. ka B.P.) is remarkable.

[29] The Early Weichselian glaciation described by *Mangerud et al.* [1996, 1998] as a major glacial

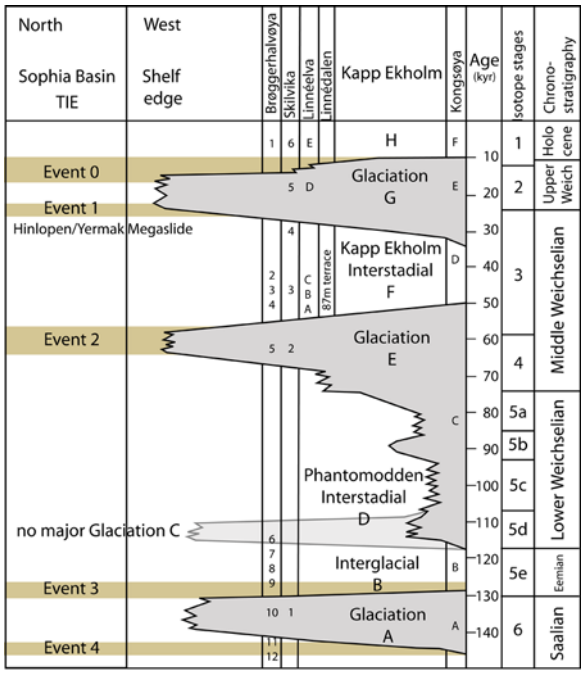

Figure 8. Terrigeneous input events (TIEs) of the Sophia Basin north of Spitsbergen and revised glaciation curve for Svalbard during the last glacial cycle (modified after *Mangerud et al.* [1998] with permission from Elsevier; for location names and associated numbering, see *Mangerud et al.* [1998, and references therein]).

advance to the shelf edge is not documented as a TIE in our sediment cores. These results are in accordance with findings of *Knies et al.* [1999, 2000, 2001] from the northern Barents Sea Margin and Severnaya Zemlya. The synthesis of terrestrial evidence for an Early Weichselian major ice sheet advance on Svalbard is essentially based on the site interpretation at Kapp Ekholm. This site is situated in central Spitsbergen. There, the identification of this Early Weichselian till is based upon intrasite correlation of outcrops [cf. *Mangerud et al.*, 1998]. The wider correlation of the corresponding marine sediments of the so-called Phantom Odden Interstadial is based on luminescence dates. This correlation appears tentative, since the luminescence dates do not show significantly different values for marine sediments of the Interglacial B (Eemian) and the Phantomodden Interstadial that would enclose a diamicton from glacial advances [cf. *Mangerud et al.*, 1998; *Forman*, 1999]. On Kongsøya, a site of the main deposition center of the SBIS, there is no indication for an Early Weichselian ice sheet [*Ingólfsson et al.*, 1995].

[30] Therefore we question the existence of an Early Weichselian glaciation on Svalbard (Glaciation C of the Svalbard glaciation curve [cf. *Mangerud et al.*, 1998]) that is still included in the recent view of the Weichselian glaciation history [cf. *Svendsen et al.*, 2004] and the associated Phantom Odden Interstadial as a separate unit. Owing to the fact that an Early Weichselian glaciation is recorded in other (remote) terrestrial archives as well as in sea level changes [e.g., *Lambeck et al.*, 2002], we rather see Svalbard being still inundated following the Late Saalian glaciation and/or being too warm during the MIS 5e-c. Northern Svalbard was probably not experiencing an extensive glaciation between 115 and 100 ka B.P. and was rather moderately glaciated during MIS5 as indicated by slightly elevated Zr/Ca ratios (Figure 4). This conclusion is supported by the terrestrial records in Brøggerhalvøya, Kapp Ekholm, Skilvika, Hidalen (Kongsøya) depending on their interpretation [see *Mangerud et al.*, 1998, and references therein] as well as geological evidence from marine records [e.g., *Knies et al.*, 2000, 2001] and, thus, revises the current glaciation curve of Svalbard [*Mangerud et al.*, 1998] (Figure 8). In analog to Severnaya Zemlya [*Möller et al.*, 2006], the Svalbard archipelago probably constituted glaciation nuclei for the subsequent growths of the SBIS during the MIS 5 and for the preceding and proceeding glaciations.

[31] The occurrence of orderly layered expandable minerals (OLEMs) within Event 1 [cf. *Vogt et al.*, 2001] has been attributed to hot shales cropping out on the Spitsbergenbanken. The plume of the interpreted plumite originated from the Storfjord ice stream and can be traced in sediment cores at declining water depths west of Spitsbergen and around the Yermak Plateau. The associated interval in our cores corresponds to TIE 1 (Figure 3). The same Event 1 (TIE 1) sediments have been found in PS2138 from the Franz-Victoria Trough (FVT) [*Knies and Stein*, 1998]. This core is positioned in shallower water depths (862 m) excluding a plume transport via Fram Strait. Given the fact that the hot shales have been only reported to crop out on the Spitsbergenbanken and that their sediments reached from there the FVT in eastern direction, the Spitsbergenbanken must have been a glaciation nucleus [cf. *Howell et al.*, 2000] for the Late Weichselian glaciation in that area [cf. *Mangerud et al.*, 1998; *Svendsen et al.*, 2004]. The Barents Sea shelf further east must have been covered by the sea before 24 cal. ka B.P. to allow a plume transport into the FVT. Additionally, a sea level drop [cf. *Lambeck et al.*, 2002] probably in concert

with a developing fore bulge [cf. *Winkelmann and Stein*, 2007] would be necessary to expose the Spitsbergenbanken subaerially to allow for extensive ice sheet growth. Main ice deposition centers reconstructed from postglacial emergence [cf. *Landvik et al.*, 1998, and references therein] would be thus less reliable. They then rather tell us about lithospheric rebound than ice loading history. Alternatively, TIE 1 has little plumite character. In this view an excessive iceberg drift transported the terrigenous input signal along the paleo-West Spitsbergen Current from the Storfjord to the FVT.

[32] The apparent synchronity of IRD events in North Atlantic's sediments and the possible link to short time sea level fluctuations [cf. *McCabe and Clark*, 1998] might be alternatively explained by a far-reaching iceberg drift in the North Atlantic realm. The differences in timing between west Svalbard and north Svalbard input sources stands against synchronous, sea level–induced iceberg discharges on Svalbard. The IRD record (according to *Grobe* [1987]) seems decoupled from the TIEs in large intervals as seen in our core records (Figures 4 and 5). This, again, points to a prominent iceberg drift probably from the Nordic Seas. The associated meridional surface circulation pattern with a counterclockwise iceberg drift has been reported for the glacial buildup phases throughout the last ~200 ka [*Hebbeln et al.*, 1994, 1998; *Dokken and Hald*, 1996; *Knies et al.*, 2000; *Hald et al.*, 2001; *Spielhagen et al.*, 2004] for the cooler stages of the Holocene [*Pirrung et al.*, 2002] and for the OLEM events during TIE 1 and upper MIS 5 [cf. *Vogt et al.*, 2001].

[33] Early MIS 3, for example, is characterized by an increase of carbonate contents, rather low and low variable TOC contents and C/N ratios. High IRD contents point toward increased glacial activity throughout the early and middle MIS 3. Both key cores (PS66/309-1 KAL and PS66/308-3 SL) show three maxima in early MIS 3. They all exhibit a similar pattern and point toward a well-developed cyclicity of the IRD signal during this time. The cyclic IRD peaks that characterize the MIS 3 might correspond to the Daansgaard-Oeschger Events (DO events) in Greenland ice cores and their relation to the Heinrich events (H events) that are well described in marine records of the North Atlantic and Nordic Seas [e.g., *Bond et al.*, 1992; *Voelker*, 1999; *Voelker et al.*, 2000; *Mix et al.*, 2001]. In contrast to sediment cores off Greenland [*Kierdorf*, 2006], these events are not imprinted on the TOC records in our cores. One probable explanation is the drift of icebergs coming from Greenland with the paleo-WSC toward the southwestern Sophia Basin during MIS 3. Both the carbonate record and the cyclic IRD peaks point to this meridional circulation condition [cf. *Vogt et al.*, 2001]. There are 7 distinct IRD events during the time window of D/O 6–18, including H4–6 in our cores. H6 as well as H2 may be recorded as TIEs in the Zr/Ca record (Figure 4). However, a local source appears not probable for the remaining IRD events since they are not reflected as TIEs.

7. Conclusions

[34] 1. The Sophia Basin is characterized by at least 5 terrigenous input events (TIEs) during the last 6 marine isotope stages.

[35] 2. Each event is associated with intensive glacial activity on Svalbard reflecting either a major glacial advance or a deglaciation (or both for the Mid Weichselian glaciation).

[36] 3. They exhibit highest densities and associated acoustic impedances and are thus excellent reflectors in the sediment penetrating acoustic imaging of sedimentary structures, best seen in the PARASOUND data. With the establishment of our chronology they can be used for regional acoustic stratigraphy.

[37] 4. The TIEs are initially characterized by elevated concentrations of terrigenous organic material, lowest to missing carbonate contents and associated peaks in C/N and Zr/Ca ratios.

[38] 5. The offset between C/N and TOC peaks to Zr/Ca reflects the different origin (west Svalbard and north Svalbard, respectively).

[39] 6. Thus, west Svalbard appears more susceptible to glacial inception than north Svalbard.

[40] 7. The Early Weichselian glaciation is not recorded as a major ice sheet advance to the shelf break in our sediment cores.

[41] 8. Therefore, we question the existence of this major glaciation on Svalbard.

Acknowledgments

[42] This study was funded by the German Research Foundation (DFG, STE 412/17). We are thankful to the scientific shipboard party and the captain and crew of the R/V *Polarstern* during ARK-XX/3. We thank Henk deHaas and an anonymous reviewer for criticism and comments on an earlier version of this manuscript.

References

Andersen, E. S., T. M. Dokken, A. Elverhøi, A. Solheim, and I. Fossen (1996), Late Quaternary sedimentation and glacial history of the western Svalbard margin, *Mar. Geol.*, *133*, 123–156, doi:10.1016/0025-3227(96)00022-9.

Bond, G. C., and R. Lotti (1995), Iceberg discharges into the North Atlantic on millennial time scales during the last glaciation, *Science*, *267*, 1005–1010, doi:10.1126/science.267.5200.1005.

Bond, G. C., et al. (1992), Evidence for massive iceberg discharges in the North Atlantic Ocean during the last glacial period, *Nature*, *360*, 245–249, doi:10.1038/360245a0.

Dokken, T. M., and M. Hald (1996), Rapid climatic shifts during isotope stages 2–4 in the Polar North Atlantic, *Geology*, *24*(7), 599–602, doi:10.1130/0091-7613(1996)024<0599:RCSDIS>2.3.CO;2.

Duplessy, J.-C. (1978), Isotope studies, in *Climatic Change*, edited by J. R. Gribbin, pp. 46–67, Cambridge Univ. Press, Cambridge, U. K.

Forman, S. L. (1999), Infrared and red stimulated luminescence dating of Late Quaternary near-shore sediments from Spitsbergen, Svalbard, Arctic, *Arct. Alp. Res.*, *31*(1), 34–49, doi:10.2307/1552621.

Fronval, T., E. Jansen, J. Bloemendal, and S. Johnson (1995), Oceanic evidence for coherent fluctuations in Fennoscandian and Laurentide ice sheets on millennium time scales, *Nature*, *374*, 443–446, doi:10.1038/374443a0.

Grobe, H. (1987), A simple method for determination of ice rafted debris in sediment cores, *Polarforschung*, *57*(3), 123–126.

Hald, M., T. Dokken, and G. Mikalsen (2001), Abrupt climatic change during the last interglacial–glacial cycle in the polar North Atlantic, *Mar. Geol.*, *176*, 121–137, doi:10.1016/S0025-3227(01)00158-X.

Hebbeln, D., T. Dokken, E. S. Andersen, M. Hald, and A. Elverhøi (1994), Moisture supply for northern ice-sheet growth during the Last Glacial Maximum, *Nature*, *370*, 357–359, doi:10.1038/370357a0.

Hebbeln, D., R. Henrich, and K. H. Baumann (1998), Paleoceanography of the last Interglacial/Glacial Cycle in the Polar North Atlantic, *Quat. Sci. Rev.*, *17*, 125–153, doi:10.1016/S0277-3791(97)00067-X.

Heinrich, H. (1988), Origin and consequences of cyclic ice rafting in the northeast Atlantic Ocean during the past 130,000 years, *Quat. Res.*, *29*, 142–152, doi:10.1016/0033-5894(88)90057-9.

Hodell, D. A., O. E. Romero, U. Roehl, J. E. Channell, and Experiment 303 Shipboard Scientific Party (2005), Detrital carbonate (Heinrich-type) layers during glacial stages of the Brunhes chronozone at IODP Site 1308 (re-occupation of DSDP Site 609), *Eos Trans. AGU*, *86*(52), Fall Meet. Suppl., Abstract PP33A-1553.

Howell, D., M. J. Siegert, and J. A. Dowdeswell (2000), Modelling the influence of glacial isostasy on Late Weichselian ice-sheet growth in the Barents Sea, *J. Quat. Sci.*, *15*(5), 475–486, doi:10.1002/1099-1417(200007)15:5<475::AID-JQS523>3.0.CO;2-I.

Ingólfsson, Ó., F. Rögnvaldsson, H. Bergsten, L. Hedenäs, G. Lehmdal, J. L. Lirio, and H. P. Sejrup (1995), Late Quaternary glacial and environmental history of Kongsøya, Svalbard, *Polar Res.*, *14*, 123–129, doi:10.1111/j.1751-8369.1995.tb00685.x.

Jakobsson, M., N. Z. Cherkis, J. Woodward, R. Macnab, and B. Coakley (2000), New grid of Arctic bathymetry aids scientists and mapmakers, *Eos Trans. AGU*, *81*(9), 89, doi:10.1029/00EO00059.

Jokat, W. (Ed.) (2000), *The Expedition RKTIS-XV/2 of Polarstern in 1999*, *Ber. Polar- Meeresforsch.*, *368*, 128 pp., Alfred Wegener Inst., Bremerhaven, Germany.

Kierdorf, C. (2006), Variability of organic carbon along the ice-covered polar continental margin of East Greenland, Ph.D. thesis, 241 pp., Univ. of Bremen, Bremen, Germany.

Knies, J., and R. Stein (1998), New aspects of organic carbon deposition and its paleoceanographic implications along the northern Barents Sea margin during the last 30,000 years, *Paleoceanography*, *13*(4), 384–394, doi:10.1029/98PA01501.

Knies, J., C. Vogt, and R. Stein (1999), Late Quaternary growth and decay of the Svalbard-Barents Sea ice sheet and paleoceanographic evolution in the adjacent Arctic ocean, *Geo Mar. Lett.*, *18*, 195–202, doi:10.1007/s003670050068.

Knies, J., N. R. Nowaczyk, C. Müller, C. Vogt, and R. Stein (2000), A multiproxy approach to reconstruct the environmental changes along the Eurasian continental margin over the last 150 000 years, *Mar. Geol.*, *163*, 317–344, doi:10.1016/S0025-3227(99)00106-1.

Knies, J., H. P. Kleiber, N. Nowaczyk, J. Mathiessen, C. Muller, F. Niessen, R. Stein, and D. Weiel (2001), Marine ice-rafted debris records constrain maximum extent of Saalian and Weichselian ice-sheets along the northern Eurasian Margin, *Global Planet. Change*, *31*, 45–64, doi:10.1016/S0921-8181(01)00112-6.

Knies, J., M. Hald, H. Ebbesen, U. Mann, and C. Vogt (2003), A deglacial–middle Holocene record of biogenic sedimentation and paleoproductivity changes from the northern Norwegian continental shelf, *Paleoceanography*, *18*(4), 1096, doi:10.1029/2002PA000872.

Lambeck, K., Y. Yokoyama, and T. Purcell (2002), Into and out of the Last Glacial Maximum: Sea-level change during Oxygen Isotope Stages 3 and 2, *Quat. Sci. Rev.*, *21*, 343–360, doi:10.1016/S0277-3791(01)00071-3.

Landvik, J. Y., S. Bondevik, A. Elverhøi, W. Fjeldskaar, J. Mangerud, O. Salvigsen, M. J. Siegert, J. I. Svendsen, and T. O. Vorren (1998), The last glacial maximum of Svalbard and the Barents sea area: Ice sheet extent and configuration, *Quat. Sci. Rev.*, *17*, 43–75, doi:10.1016/S0277-3791(97)00066-8.

Lisiecki, L. E., and M. E. Raymo (2005), A Pliocene-Pleistocene stack of 57 globally distributed benthic δ^{18}O records, *Paleoceanography*, *20*, PA1003, doi:10.1029/2004PA001071.

MacAyeal, D. R. (1993), Binge/Purge oscillations of the Laurentide ice sheet as the cause of the North Atlantic's Heinrich events, *Paleoceanography*, *8*, 775–784, doi:10.1029/93PA02200.

Mangerud, J., E. Jansen, and J. Landvik (1996), Late Cenozoic history of the Scandinavian and Barents Sea ice sheets, *Global Planet. Change*, *12*, 11–26, doi:10.1016/0921-8181(95)00009-7.

Mangerud, J., T. Dokken, D. Hebbeln, B. Heggen, Ó. Ingólfsson, J. Y. Landvik, V. Mejdahl, J. I. Svendsen, and T. O. Vorren (1998), Fluctuations of the Svalbard-Barents Sea ice sheet during the last 150 000 years, *Quat. Sci. Rev.*, *17*, 11–42, doi:10.1016/S0277-3791(97)00069-3.

Martinson, D. G., N. G. Pisias, J. D. Hays, J. Imbrie, T. C. Moore, and N. J. Shackleton (1987), Age dating and the orbital theory of the ice ages: Development of a high-resolution 0 to 300,000 years chronostratigraphy, *Quat. Res.*, *27*, 1–27, doi:10.1016/0033-5894(87)90046-9.

McCabe, A. M., and P. U. Clark (1998), Ice-sheet variability around the North Atlantic Ocean during the last glaciation, *Nature*, *392*, 373–377, doi:10.1038/32866.

Mix, A. C., E. Bard, and R. Schneider (2001), Environmental processes of the ice age: Land, ocean, glaciers (EPILOG), *Quat. Sci. Rev.*, *20*, 627–657, doi:10.1016/S0277-3791(00)00145-1.

Möller, P., et al. (2006), Severnaya Zemlya, Arctic Russia: A nucleation area for Kara Sea ice sheets during the Middle to Late Quaternary, *Quat. Sci. Rev.*, *25*, 2894–2936, doi:10.1016/j.quascirev.2006.02.016.

Nørgaard-Pedersen, N., R. F. Spielhagen, J. Thiede, and H. Kassens (1998), Central Arctic surface ocean environment during the past 80,000 years, *Paleoceanography*, *13*(2), 193–204, doi:10.1029/97PA03409.

Ottesen, D., J. A. Dowdeswell, and L. Rise (2005), Submarine landforms and the reconstruction of fast-flowing ice streams within a large Quaternary ice sheet: The 2500-km-long Norwegian-Svalbard margin (57°–80°N), *Geol. Soc. Am. Bull.*, *117*(7/8), 1033–1050, doi:10.1130/B25577.1.

Pirrung, M., D. Fütterer, H. Grobe, J. Matthiessen, and F. Niessen (2002), Magnetic susceptibility and ice-rafted debris in surface sediments of the Nordic Seas: Implications for Isotope Stage 3 oscillations, *Geo Mar. Lett.*, *22*, 1–11, doi:10.1007/s00367-002-0090-1.

Richter, T. O., S. van der Gaast, R. Koster, A. Vaars, R. Gieles, H. C. de Stigter, H. De Haas, and T. C. E. van Weering (2006), The Avaatech XRF Core Scanner: Technical description and applications to NE Atlantic Sediments, in *New Techniques in Sediment Core Analysis*, edited by R. G. Rothwell, *Geol. Soc. Spec. Publ.*, *267*, 39–50.

Schäfer, C. (2005), Untersuchungen zu Menge und Zusammensetzung des Organischen Kohlenstoffs in spätquartären Sedimenten des Yermak-Plateaus (Arktischer Ozean) und Umweltbedingungen, Master thesis, 105 pp., Univ. of Trier, Trier, Germany.

Schauer, U., E. Fahrbach, S. Osterhus, and G. Rohardt (2004), Arctic warming through Fram Strait: Ocean heat transport from 3 years of measurement, *J. Geophys. Res.*, *109*, C06026, doi:10.1029/2003JC001823.

Schubert, C. J., and S. E. Calvert (2001), Nitrogen and carbon isotopic composition of marine and terrestrial organic matter in Arctic Ocean sediments: Implications for nutrient utilization and organic matter composition, *Deep Sea Res., Part I*, *48*, 789–810, doi:10.1016/S0967-0637(00)00069-8.

Spielhagen, R. F., K. H. Baumann, H. Erlenkeuser, N. R. Nowaczyk, N. Nørgaard-Pedersen, C. Vogt, and D. Weiel (2004), Arctic Ocean deep-sea record of northern Eurasian ice sheet history, *Quat. Sci. Rev.*, *23*, 1455–1483, doi:10.1016/j.quascirev.2003.12.015.

Stein, R. (Ed.) (2005), Scientific cruise report of the Arctic Expedition ARK-XX/3 of RV "Polarstern" in 2004: Fram Strait, Yermak Plateau and East Greenland Continental Margin, *Rep. Polar Mar. Res.*, *517*, Alfred Wegener Inst., Bremerhaven, Germany.

Stein, R., and R. W. Mcdonald (Eds.) (2004), *The Organic Carbon Cycle in the Arctic Ocean*, 363 pp., Springer, Berlin.

Stein, R., H. Grobe, and M. Wahsner (1994), Organic carbon, carbonate, and clay mineral distributions in eastern central Arctic Ocean surface sediments, *Mar. Geol.*, *119*, 269–285, doi:10.1016/0025-3227(94)90185-6.

Svendsen, J. I., et al. (2004), Late Quaternary ice sheet history of northern Eurasia, *Quat. Sci. Rev.*, *23*, 1229–1271, doi:10.1016/j.quascirev.2003.12.008.

Thompson, W. G., and S. L. Goldstein (2006), A radiometric calibration of the SPECMAP timescale, *Quat. Sci. Rev.*, *25*, 3207–3215, doi:10.1016/j.quascirev.2006.02.007.

Tjallingii, R., U. Röhl, M. Kölling, and T. Bickert (2007), Influence of the water content on X-ray fluorescence core-scanning measurements in soft marine sediments, *Geochem. Geophys. Geosyst.*, *8*, Q02004, doi:10.1029/2006GC001393.

Voelker, A. H. L. (1999), Zur Deutung der Dansgaard-Oeschger Ereignisse in ultra-hochauflösenden Sedimentprofilen aus dem Europäischen Nordmeer, D.Sc. dissertation, *Ber. Inst. Geowiss. 9*, 278 pp., Univ. of Kiel, Kiel, Germany.

Voelker, A. H. L., P. M. Grootes, M. J. Nadeau, and M. Sarnthein (2000), Radiocarbon levels in the Iceland Sea from 25–53 kyr and their link to the earth's magnetic field intensity, *Radiocarbon*, *42*, 437–452.

Vogt, C., J. Knies, R. F. Spielhagen, and R. Stein (2001), Detailed mineralogical evidence for two nearly identical glacial/deglacial cycles and Atlantic water advection to the Arctic Ocean during the last 90,000 years, *Global Planet. Change*, *31*, 23–44, doi:10.1016/S0921-8181(01)00111-4.

Winkelmann, D. (2003), Reconstruction of recent and late Holocene sedimentation processes on the continental shelf west off Spitsbergen, M.S. thesis, 156 pp., TU Bergakad. Freiberg, Freiberg, Germany.

Winkelmann, D. (2007), Sediment dynamics of megaslides along the Svalbard continental margin and the relation to paleoenvironmental changes and climate history, Ph.D. thesis, 183 pp., Univ. of Bremen, Bremen, Germany.

Winkelmann, D., and J. Knies (2005), Recent distribution and accumulation of organic carbon on the continental margin west off Spitsbergen, *Geochem. Geophys. Geosyst.*, *6*, Q09012, doi:10.1029/2005GC000916.

Winkelmann, D., and R. Stein (2007), Triggering of the Hinlopen/Yermak Megaslide in relation to paleoceanography and climate history of the continental margin north of Spitsbergen, *Geochem. Geophys. Geosyst.*, *8*(6), Q06018, doi:10.1029/2006GC001485.

Winkelmann, D., W. Jokat, F. Niessen, R. Stein, and A. Winkler (2006a), Age and extent of the Yermak Slide north of Spitsbergen, Arctic Ocean, *Geochem. Geophys. Geosyst.*, *7*, Q06007, doi:10.1029/2005GC001130.

Winkelmann, D., W. Jokat, F. Niessen, R. Stein, and A. Winkler (2006b), Dynamic and timing of the Yermak/Hinlopen Slide, Arctic Ocean, paper presented at European Geosciences Union General Assembly 2006, Vienna, Austria, 2–7 April.

Winkelmann, D., W. H. Geissler, J. Schneider, R. Stein, and H.-W. Schenke (2008), Dynamic and timing of the Hinlopen/Yermak Megaslide north of Spitsbergen, Arctic Ocean, *Mar. Geol.*, *250*, 34–50, doi:10.1016/j.margeo.2007.11.013.